

Low-Dissipation Data Bus via Coherent Quantum Dynamics

Dylan Lewis,^{1,*} João P. Moutinho,^{2,3} António Costa,⁴ Yasser Omar,^{3,5,6} and Sougato Bose¹

¹*Department of Physics and Astronomy, University College London, London WC1E 6BT, United Kingdom*

²*Instituto de Telecomunicações, Physics of Information and Quantum Technologies Group, Lisbon, Portugal*

³*Instituto Superior Técnico, Universidade de Lisboa, Lisbon, Portugal*

⁴*International Iberian Nanotechnology Laboratory, 4715-330 Braga, Portugal*

⁵*Centro de Física e Engenharia de Materiais Avançados (CeFEMA),*

Physics of Information and Quantum Technologies Group, Portugal

⁶*Portuguese Quantum Institute, Lisbon, Portugal*

The transfer of information between two physical locations is an essential component of both classical and quantum computing. In quantum computing the transfer of information must be coherent to preserve quantum states and hence the quantum information. We establish a simple protocol for transferring one- and two-electron encoded logical qubits in quantum dot arrays. The theoretical energetic cost of this protocol is calculated—in particular, the cost of freezing and unfreezing tunnelling between quantum dots. Our results are compared with the energetic cost of shuttling qubits in quantum dot arrays and transferring classical information using classical information buses. Only our protocol can manage constant dissipation for any chain length. This protocol could reduce the cooling requirements and constraints on scalable architectures for quantum dot quantum computers.

I. INTRODUCTION

Quantum dot quantum computers encode qubit states using electrons isolated in confined regions by electric fields. Efficiently transferring qubit states in these semiconductor-based architectures is a significant unresolved problem for their scalability. Recent proposals have focused on coherently shuttling the electrons [1, 2] and on transfer through multiple quantum dots using engineered tunnel couplings [3], which employs theoretical results from work in perfect state transfer [4–6].

A distinct but related question is the energetic cost of using electric currents for the transfer of information in semiconductor-based classical computation. Generating the required potential gradients is a major source of energetic cost.

Landauer’s principle states that the energy dissipated in the form of heat to erase a bit of information is $k_B T \log 2$ [7], suggesting a minimum energetic cost for computation. However, any computation can be performed reversibly [8] and the Landauer limit can in theory be surpassed. Despite further work on computing using reversible logic [9], there remain essentially no practical implementations that are both frictionless and fast. Adiabatic computing, which is slow reversible computing, has been proposed but with significant reductions in performance [10, 11]. Quantum computing, using unitary evolutions, is inherently reversible and therefore provides a possible platform for low-energy computation. The coherent manipulation of single electrons for classical computation has recently been proposed, with Moutinho et al. [12] considering the energetic advantage of using a quantum dot array with Fredkin gates to implement a full adder, raising the pertinent question of whether a

classical computer based on using small quantum systems could provide an energetic advantage for classical computation. The logical states of the qubits are one- and two-electron encodings. Motivated by this, we address the question of low-dissipation quantum buses in quantum dot architectures for quantum and classical data. In this model of a quantum data bus, linear chains of qubits can effectively transfer quantum information due to the natural evolution of an interacting Hamiltonian. In theory, quantum state transfer [4, 5] can coherently transfer information via quantum states without necessarily requiring a voltage.

Currently, computers are many orders of magnitude from the Landauer limit, with the most powerful supercomputers consuming on the order of keV to MeV per bit operation [12]. Despite the effort in reducing computational energetic costs, the fundamental limits for electron-based computing suggests that the interconnects—fixed wiring—is the *primary* factor limiting the efficiency of computation, potentially orders of magnitude more costly than computation itself [13]. Here, we address this problem directly by proposing a classical bus using coherent quantum dynamics where the energetic cost does not scale with the length of the wire. We establish a protocol for efficient transfer of an electron using perfect state transfer chains and a simple electron separation protocol. This protocol could be used for quantum computation to alleviate some cooling constraints in scalable quantum computing architectures [14]. We find the energetic cost of changing the tunnel coupling between two quantum dots and the minimum energetic cost of implementing the protocol. This is compared to our computed minimum energetic costs for shuttling and for classical data buses. We also make a note on the effect of noise in experimental quantum dot arrays.

* dylan.lewis.19@ucl.ac.uk

II. PHYSICAL MODEL

For the quantum dot chains that we consider, the logical qubit is encoded in the charge, rather than spin. The state transfer is a state $|\psi_1(t_0)\rangle$ at time t_0 , initialised on quantum dot 1 in the chain, being transferred to the last quantum dot in the chain at specific time T , $|\psi_N(T)\rangle$, with a high fidelity, $F = |\langle\psi_1(t_0)|\psi_N(T)\rangle|^2$.

We set the initial time $t_0 = 0$ and the initial state for transfer to $|\psi(0)\rangle = |\psi_1(0)\rangle \otimes |0\rangle \otimes \dots \otimes |0\rangle$. The protocol, in the simplest case, involves simply turning on interactions for specific time T and then turning off interactions. The state is then at the final site N with high fidelity.

A. Hubbard model

The general model for interacting quantum dots is an extended Hubbard Hamiltonian with both capacitive and tunnel coupling,

$$\begin{aligned} \frac{H}{\hbar} = & \sum_{i,\sigma} \varepsilon_i \hat{n}_{i,\sigma} + \sum_{i,\sigma} \Gamma_i (c_{i,\sigma}^\dagger c_{i+1,\sigma} + c_{i+1,\sigma}^\dagger c_{i,\sigma}) \\ & + \sum_{i,\sigma,\sigma'} V_i \hat{n}_{i,\sigma} \hat{n}_{i+1,\sigma'} + \sum_i U_i \hat{n}_{i,\uparrow} \hat{n}_{i,\downarrow}, \end{aligned} \quad (1)$$

where ε_i is the local field applied to quantum dot i , Γ_i is the tunnel coupling between quantum dots i and $i+1$, V_i is the capacitive coupling between quantum dots i and $i+1$, U_i is the onsite interaction at site i , $c_{i,\sigma}$ and $c_{i,\sigma}^\dagger$ are respectively the annihilation and creation operators of an electron on quantum dot i with spin σ . The number operator for electrons of spin σ is therefore $\hat{n}_{i,\sigma} = c_{i,\sigma}^\dagger c_{i,\sigma}$.

B. Simplified models

In the transfer protocol, we start with an initial state that contains either one or two electrons depending on the logical encoding used. Hence, assuming the spins of the electrons do not flip and the number of electrons is constant, significant simplifications to the general Hubbard model can be made. For a single-electron logical qubit, we simply have the tunnel-coupling term and local potential,

$$\frac{H_1}{\hbar} = \sum_{i=1}^{N-1} \Gamma_{i,i+1} (|i\rangle\langle i+1| + h.c.) + \sum_{i=1}^{N-1} \varepsilon_i |i\rangle\langle i|, \quad (2)$$

where we have defined a single-electron basis for the quantum dot chain: $|i\rangle$ indicates an electron at quantum dot i with the rest of the dots in the chain empty. The spin of the electron is assumed to be unchanged throughout the protocol. The model is more complex for the two electron encoding, we introduce a two-electron state $|i,j\rangle$,

with an up spin electron at site i and a down spin electron at site j . There are N sites in the set S . The basis can therefore be labelled by $p \in S \times S = \{(i,j) \mid i \in S \text{ and } j \in S\}$, giving length N^2 and can be constructed as $|p\rangle = |i,j\rangle = c_{i,\uparrow}^\dagger c_{j,\downarrow}^\dagger |0\rangle$. The Hamiltonian matrix elements are thus

$$H_{p,p'} = \langle 0 | c_{j,\downarrow} c_{i,\uparrow} H c_{i',\uparrow}^\dagger c_{j',\downarrow}^\dagger | 0 \rangle \quad (3)$$

The anti-commutation relations of fermions must be considered, $\{c_{i,\sigma}, c_{j,\sigma'}\} = \{c_{i,\sigma}^\dagger, c_{j,\sigma'}^\dagger\} = 0$ and $\{c_{i,\sigma}, c_{j,\sigma'}^\dagger\} = \delta_{i,j} \delta_{\sigma,\sigma'}$. With this careful choice of basis, such that the order of creation operators for the up spin and down spin are not permuted, we find

$$\begin{aligned} \frac{H_2}{\hbar} = & \sum_{i,j=1}^{N-1} \left[\Gamma_{i,i+1} (|i,j\rangle\langle i+1,j| + h.c.) \right. \\ & + \Gamma_{j,j+1} (|i,j\rangle\langle i,j+1| + h.c.) \\ & + U \delta_{i,j} |i,j\rangle\langle i,j| \\ & + V (\delta_{i,j+1} + \delta_{i+1,j}) |i,j\rangle\langle i,j| \\ & \left. + (\varepsilon_i + \varepsilon_j) |i,j\rangle\langle i,j| \right], \end{aligned} \quad (4)$$

where $\delta_{i,j}$ is the Kronecker delta and we have assumed the onsite interaction, U , and capacitive coupling, V , are the same for all quantum dots. These Hamiltonians live in significantly smaller Hilbert spaces than the full Hubbard model, which is a space that increases exponentially with number of quantum dots N . On the other hand, for $H_1 \in \mathcal{H}_1$ and $H_2 \in \mathcal{H}_2$, we have $\dim(\mathcal{H}_1) \sim N$ and $\dim(\mathcal{H}_2) \sim N^2$, which are both significantly simpler to simulate.

III. STATE TRANSFER WITH A SINGLE ELECTRON

The single-electron Hamiltonian of Eq. (2) is equivalent to the Hamiltonian of the single-excitation subspace dynamics of the XY model—a well-studied model for state transfer [6]. We consider schemes that limit the use of ε_i local fields as it would increase the energetic cost of the protocol. The energetic costs of both this protocol and of a classical information bus, are addressed in Section V.

In fact, perfect state transfer can be achieved directly with the XY model in a number of ways that do not require local fields. Engineering the spin-chain tunnel couplings can lead to perfect state transfer. This can be seen by rewriting Eq. (2) in matrix form,

$$\frac{H_1}{\hbar} = \begin{pmatrix} \varepsilon_1 & \Gamma_{1,2} & 0 & \cdots & & \\ \Gamma_{1,2} & \varepsilon_2 & \Gamma_{2,3} & 0 & \ddots & \\ 0 & \Gamma_{2,3} & \varepsilon_3 & \Gamma_{3,4} & 0 & \ddots \\ \vdots & 0 & \Gamma_{3,4} & \varepsilon_4 & \Gamma_{4,5} & \ddots \\ & \ddots & \ddots & \ddots & \ddots & \ddots \end{pmatrix}. \quad (5)$$

First, note that the raising and lowering operators of a large spin with $s = (N - 1)/2$ act on basis states as $\hat{S}_\pm |s, m\rangle = \sqrt{s(s+1) - m(m \pm 1)} |s, m \pm 1\rangle$. For given s and quantum dot $1 \leq i \leq N$, we find $m = i - 1 - s$. Rotations of the spin can be induced by S_x , which is the generator of rotations about the x axis in $\text{SO}(3)$, giving $R_x(\theta) = e^{-iS_x\theta}$. With the relationships above, we see that H_1 is equivalent to $2S_x = S_+ + S_-$ by setting $\varepsilon_i = 0$ for all i and

$$\Gamma_{i,i+1} = \sqrt{s(s+1) - m(m+1)} \quad (6)$$

$$= \sqrt{i(N-i)}. \quad (7)$$

After a time $T = \pi/2$, which gives unitary evolution $U(\pi/2) = e^{-iH_1\pi/2\hbar} = e^{-iS_x\pi}$, a rotation of π around the x axis has been induced. This takes the initial state $|1\rangle$ to the final state $|N\rangle$. Thus performing perfect state transfer in time $T \sim N$, where the tunnel coupling has been scaled such that the largest coupling is 1.

We can also use the superexchange where the two end qubits are weakly coupled to a relatively strongly-coupled many-body quantum system [15–18]. In this case, the many-body quantum system is the central quantum dots of the chain. While the fidelity of state transfer is high, the superexchange is very slow: if the coupling between the central quantum dots is such that $\Gamma_{i,i+1} \sim 1$, and the coupling of the first and final quantum dots to the central chain is $\Gamma_{1,2} = \Gamma_{N-1,N} = \epsilon$, where $\epsilon \ll 1$, then the transfer time is $T \sim 1/\epsilon^2$. Slow transfer is undesirable for scalable and fast computational architectures because it would require a slow clock frequency.

IV. STATE TRANSFER WITH TWO ELECTRONS

State transfer for two electrons is less straight forward. Although too slow for an architecture proposal, we note that transfer using the superexchange is still possible with two electrons.

Realising perfect state transfer in the same way as the single electron case, with engineered spin chains replicating S_x for a large spin s , is not possible for non-zero U and V . All diagonal terms would have to be constant (or zero). In the case of two electrons, we would require

$$U\delta_{i,j} + V(\delta_{i,j+1} + \delta_{i+1,j}) + \varepsilon_i + \varepsilon_j = d, \quad (8)$$

for all i and j . If we consider $|i - j| > 1$, ε_i must be the same for all i . Thus, $U = V = 0$ is required for all diagonal elements to be equal. In this case, we could then use the same tunnel couplings as the single electron case and have two non-interacting electrons that both separately perform perfect state transfer at the same time. If $U \ll \Gamma_{\min}$, where Γ_{\min} is the smallest coupling $\Gamma_{1,2}$, we have pretty good (not perfect) state transfer—which, given that this work is also motivated by low-dissipation classical computing, would be useful if it is experimentally feasible. For example, a chain of 16 quantum dots,

with $U = \Gamma_{\min}/10$, has a fidelity of state transfer of greater than 0.9.

We propose a protocol that first involves separating the electrons and then transferring one electron at a time along an engineered chain with perfect state transfer before recombination.

A. Two electrons and two quantum dots

The dynamics of two electrons with two quantum dots can be tuned such that there is high fidelity of electron separation, so one electron on each dot. Perfect state transfer could occur with two electrons on two quantum dots if the Hamiltonian for the evolution of the states—the adjacency matrix of the graph with additional diagonal terms—can be written as

$$\frac{H}{\hbar} = \Gamma \begin{pmatrix} 0 & 1 & 1 & 0 \\ 1 & 0 & 0 & 1 \\ 1 & 0 & 0 & 1 \\ 0 & 1 & 1 & 0 \end{pmatrix} + d\mathbb{1}, \quad (9)$$

where d would have no effect on the evolution, see Fig. 1(a) for the graph. The analysis can be simplified for certain initial states. The states $|1, 2\rangle$ and $|2, 1\rangle$ can be considered together because the quantum walk evolution, $U = e^{-iHt/\hbar}$, is symmetric with respect to these states if we start from $|1, 1\rangle$ or $|2, 2\rangle$, see Fig. 1(b). This gives the adjacency matrix

$$A = \sqrt{2}\Gamma\hbar \begin{pmatrix} 0 & 1 & 0 \\ 1 & 0 & 1 \\ 0 & 1 & 0 \end{pmatrix}, \quad (10)$$

which is equal to $2\Gamma S_x$, where S_x is the x spin operator for an $s = 1$ boson. Thus, if we assume no detuning between sites, A is equivalent to a rotation around the x axis and, as before, perfect state transfer occurs in time $T = \pi\hbar/2\Gamma$.

If we detune the final state $|2, 2\rangle$ from the rest, we suppress the coherent transfer to this site. The dynamics now lead to a high fidelity transfer between $|1, 1\rangle$ and a superposition of $|1, 2\rangle$ and $|2, 1\rangle$, precisely the state required for coherent electron separation. To demonstrate the cause of the suppression, consider only the interaction of the superposition of the separated electrons with the $|2, 2\rangle$ state, so a two-state system with one of the states detuned by δ . Relabelling the basis states $|0\rangle$ and $|1\rangle$, we have the Hamiltonian

$$\frac{H}{\hbar} = \Gamma\sigma_x - \frac{\delta}{2}\sigma_z + \frac{\delta}{2}\mathbb{1}, \quad (11)$$

where σ_x and σ_z are the standard Pauli matrices. We can neglect the identity term as it only adds a global phase. The evolution of the state is therefore

$$U(t) = e^{-i(\Gamma\sigma_x - \frac{\delta}{2}\sigma_z)t} \quad (12)$$

$$= \cos(nt)\mathbb{1} + i\frac{\delta}{2n}\sin(nt)\sigma_z - i\frac{\Gamma}{n}\sin(nt)\sigma_x, \quad (13)$$

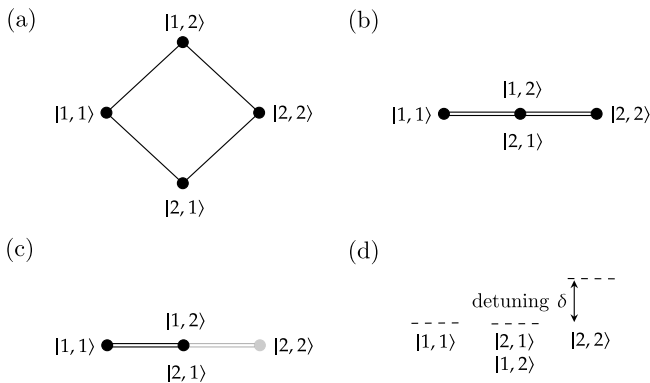


FIG. 1. Graphs of states in various representations: (a) all two-electron two quantum dot states are considered where the electrons have opposite spins, (b) simplification of the graph due to symmetry and initial states; (c) state $|2, 2\rangle$ is suppressed due to detuning represented in (d).

where $n = \sqrt{\Gamma^2 + (\delta/2)^2}$. When $\delta = m\Gamma$ with m an integer larger than 1, the σ_x term is suppressed by $1/\sqrt{1 + \frac{m^2}{4}}$. For $m \gg 1$ we have a suppression of $\sim 2/m$ for the rotation term. This leads to a reduction in the fidelity of oscillations from $|0\rangle$ to $|1\rangle$ by approximately $4/m^2$. Typical values for electron interaction and capacitive coupling are $U = 20\Gamma$ and $V = 10\Gamma$, where Γ is the tunnel coupling between the two quantum dots [19, 20]. Applying a local field $\varepsilon_2 = 10\Gamma$ to only the second quantum dot, detunes the state $|2, 2\rangle$ by $\delta = 20\Gamma$, while the energy of the states $|1, 1\rangle$, $|1, 2\rangle$, and $|2, 1\rangle$ are all equal. Using the analysis above, we should therefore find a reduction of the fidelity, leading to the $|2, 2\rangle$, state of approximately 0.01. Numerically, we find a maximum fidelity of separation for the electrons of 0.993, see Fig. 2. The fidelity can be made higher if we use quantum dots with no capacitive coupling, so $V = 0$, and a local field $\varepsilon_2 = 20\Gamma$, which keeps the energy of the other states equal. The detuning is now $\delta = 40\Gamma$, giving an analytical fidelity loss of approximately 0.0025, which is very close to what we find numerically: a fidelity of separation of 0.998. The time for the electron separation is that of oscillations in a two state-system with interaction strength $\sqrt{2}\Gamma$ —the factor of $\sqrt{2}$ is because there are actually two states $|1, 2\rangle$ and $|2, 1\rangle$ and therefore two paths between $|1, 1\rangle$ to other node of the effective graph. Electron separation therefore occurs in time $T = \pi\hbar/2\sqrt{2}\Gamma$, which is what we find numerically.

For general U and V , to keep the energy of states $|1, 1\rangle$, $|1, 2\rangle$, and $|2, 1\rangle$ equal, we set $\varepsilon_2 = \varepsilon_1 + U - V$, giving the detuning $\delta = 2\varepsilon_2 - 2\varepsilon_1$. The larger U is, while minimising V , the larger the difference between ε_2 and ε_1 , which increases δ and therefore the fidelity of electron separation.

Once the electrons have been separated, they are coherently transferred sequentially along the central spin chain with engineered couplings, as in the single-electron

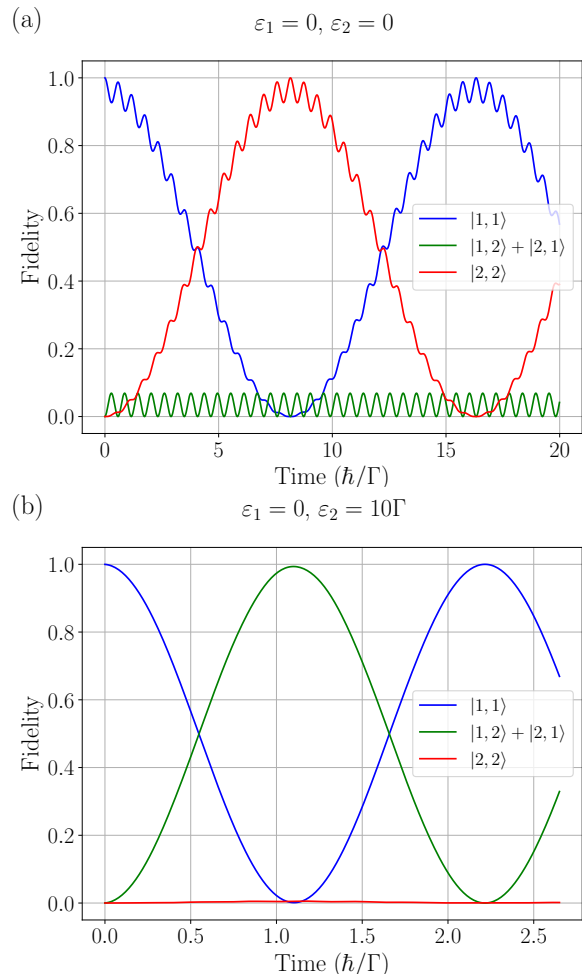


FIG. 2. Comparison of the fidelity for the separation of the electrons with $U = 20\Gamma$, $V = 10\Gamma$ (Γ is tunnel coupling) for: (a) no local fields, showing the electrons essentially remain bound together; (b) $\varepsilon_2 = 10\Gamma$, showing a maximum electron separation fidelity of 0.993.

case. In theory, this step gives unit fidelity for state transfer. Noise is discussed in Section VI. The electrons are then recombined using the inverse of the separation procedure, with essentially the same fidelity. Fig. 3 shows the steps of the protocol.

V. ENERGETIC COST

The energetic cost of both the single- and two-electron quantum buses are now considered. As a benchmark, we compare the energetic cost of shuttling electrons, and the lower bound of a data bus in a classical CPU.

With engineered couplings, the transfer of the electron is coherent. Hence the transfer itself does not require an energy source—the reason for an energetic advantage. However, the interactions must be turned on and off, which does have an energetic cost.

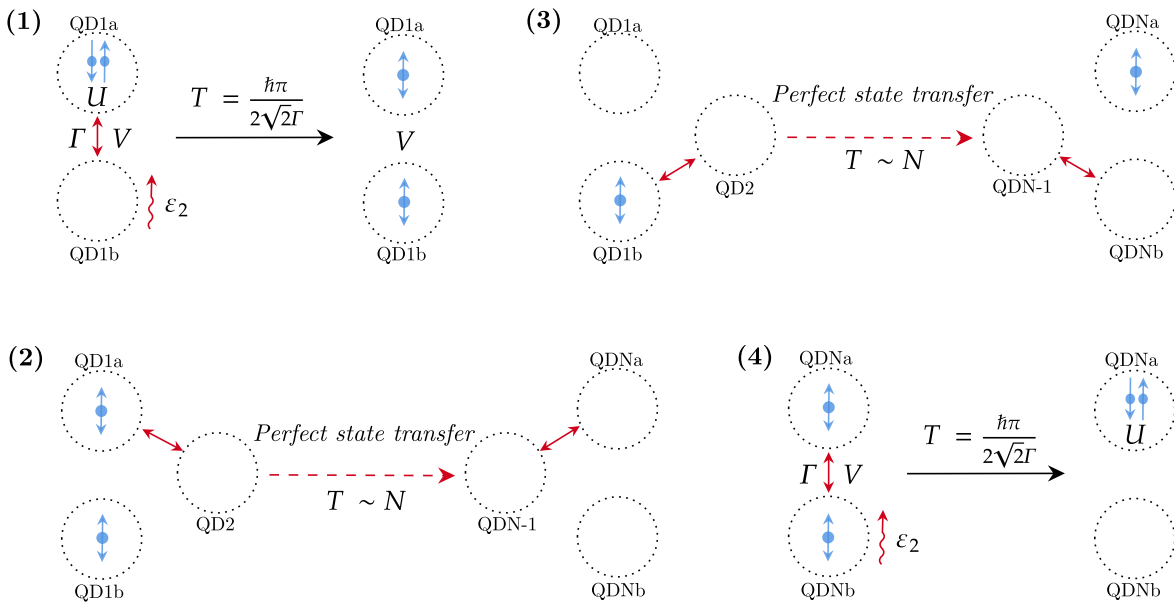


FIG. 3. Energy-efficient protocol for transfer of a two-electron logical qubit (or bit): (1) The initial state is loaded into quantum dot 1a (QD1a), and split into an equal superposition of both spins in QD1a and QD1b using electron separation protocol; (2) and (3) Perfect state transfer is used to transfer each electron individually; (4) The electrons are recombined onto QDNa.

A. Energetic cost of freezing and unfreezing interactions

We show that the energetic cost of freezing and unfreezing the interactions for a quantum dot system has an optimal energetic cost equivalent to approximately the charging energy of a quantum dot, E_C . The energetic cost of freezing and unfreezing interactions can be estimated by considering a double quantum dot with two electrons.

There are two limiting cases: the barrier potential going to zero giving one large quantum dot with two electrons; and the barrier potential being very high giving two isolated quantum dots each with harmonic potentials. In our quantum dot model, we consider the latter case, with a significant barrier. This assumption is reasonable since the preceding protocol for state transfer is in the regime $U \gg \Gamma$.

Electrons in a double quantum dot can be modelled as a biquadratic potential [19, 21–24], see Fig. 4. The Hamiltonian for two electrons is

$$H = \sum_{j=1}^2 \left[\frac{\mathbf{p}_j^2}{2m^*} + V(\mathbf{r}_j) \right] + \frac{e^2}{4\pi\epsilon_0\epsilon_r |\mathbf{r}_1 - \mathbf{r}_2|}, \quad (14)$$

where \mathbf{p}_j and \mathbf{r}_j are the momentum and position vectors of electron j in two dimensions, m^* is the effective mass, and $V(\mathbf{r})$ is the potential

$$V(\mathbf{r}) = V_0 \min [(\mathbf{r} - \mathbf{l})^2, (\mathbf{r} + \mathbf{l})^2, \mu], \quad (15)$$

where μ is the chemical potential, and the dots are located at $\pm \mathbf{l}$, a distance of $d = 2l$ apart. For large μ ,

we consider the simplification $V_S(\mathbf{r}) = \lim_{\mu \rightarrow \infty} V(\mathbf{r})$. Fig. 4 shows the form of the potential, with barrier height $V_B = V_0 l^2$ between the dots. Increasing the distance between the harmonic potentials increases the barrier height. Rather than increasing the distance, however, d is fixed and the strength of the harmonic potentials V_0 is increased. In the low temperature limit, $k_B T \ll \hbar\omega_0$, the electrons are assumed to be in their ground state. For a two-dimensional harmonic trap with $V_0 = m^* \omega_0^2 / 2$, the ground state energy, with lowest orbital momentum in the confinement, is $\hbar\omega_0$. We define a dimensionless parameter $\eta = m^* \omega_0 l^2 / \hbar$, which is the ratio of the barrier height and half the ground state energy of an electron in a harmonic trap. In this analysis, only $\eta > 1$ is considered, following from $U \gg \Gamma$. In this regime, the Heitler-London (HL) approximation is valid [24] since the quantum dots are sufficiently separated. We can thus build the two-electron ground state from single-electron harmonic ground states of model Hamiltonians of the form $h_{L/R}^{(0)} = \mathbf{p}_1^2 / 2m^* + m^* \omega_0^2 (\mathbf{r}_1 \pm \mathbf{l})^2 / 2$.

If there are no external fields, the ground state of two electrons will always be the singlet state because the spatial wave function is symmetric, i.e. exchange coupling $J \equiv E_T - E_S > 0$ [23], where $E_{T/S}$ are the triplet and singlet energies. Further to this, we will consider two electrons on the same quantum dot to calculate the charging energy E_C . The lowest energy is when both electrons can occupy the same lowest energy orbital, giving a symmetric spatial wave function, and therefore a singlet spin state. As we are not concerned with the exchange coupling, we only consider the singlet state in the following HL approximation and further analysis.

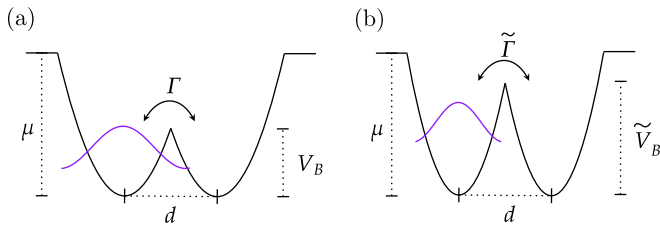


FIG. 4. One-dimensional cross section through the centre of the confining harmonic potentials that model a double quantum dot. The confinement is in two dimensions, with radial symmetry around the centre of each of the dots. The size of V_0 has been changed between (a) and (b), with (b) showing increased confinement and therefore a higher barrier.

The ground state of the harmonic potentials for the left and right quantum dots, with Hamiltonians $\hat{h}_{L/R}^{(0)}$, are

$$\varphi_{L/R}(\mathbf{r}) = \langle \mathbf{r} | L/R \rangle = \frac{1}{a\sqrt{\pi}} e^{-\frac{1}{2a^2}[(x\pm l)^2 + y^2]}, \quad (16)$$

where we have defined a Bohr radius $a = \sqrt{\hbar/m^*\omega_0}$, $\mathbf{r} = (x, y)$, and the dots are centred along the x axis. Using the HL approximation, the ground state of the two-electron double quantum dot is a symmetric spatial superposition of the electrons on different dots. We define the overlap between the adjacent harmonic potentials, $s = \langle L | R \rangle = e^{-l^2/a^2} = e^{-\eta}$. As in Ref. [25], the Hund-Mulliken (HM) approximation is used to further include the states with two electrons on the same quantum dot, the (2,0) and (0,2) states, which must also be singlet states in the ground state. The left and right basis states are rotated such that they are orthogonal, $\langle \Phi_L | \Phi_R \rangle = 0$, giving $|\Phi_{L/R}\rangle = (|L/R\rangle - g|R/L\rangle)/\mathcal{N}$ where $\mathcal{N} = \sqrt{1 - 2sg + g^2}$ and $g = (1 - \sqrt{1 - s^2})/s$, such that both \mathcal{N} and g are functions of η . In this basis, with $\Phi_{L/R}(\mathbf{r}) = \langle \mathbf{r} | \Phi_{L/R} \rangle$, the three relevant spatial wave functions are

$$\Psi_L^d(\mathbf{r}_1, \mathbf{r}_2) = \Phi_L(\mathbf{r}_1)\Phi_L(\mathbf{r}_2), \quad (17)$$

$$\Psi_R^d(\mathbf{r}_1, \mathbf{r}_2) = \Phi_R(\mathbf{r}_1)\Phi_R(\mathbf{r}_2), \quad (18)$$

$$\Psi_0^s(\mathbf{r}_1, \mathbf{r}_2) = \frac{1}{\sqrt{2}} [\Phi_L(\mathbf{r}_1)\Phi_R(\mathbf{r}_2) + \Phi_R(\mathbf{r}_1)\Phi_L(\mathbf{r}_2)], \quad (19)$$

where $\Psi_{L/R}^d(\mathbf{r}_1, \mathbf{r}_2)$ indicate the doubly occupied states (2,0) and (0,2), and $\Psi_0^s(\mathbf{r}_1, \mathbf{r}_2)$ indicates both sites being singly occupied (1,1). All these states are symmetric since the states are spin singlets.

The Hamiltonian is separable for the non-Coulomb terms: $\hat{H} = \hat{h} \otimes \mathbf{1} + \mathbf{1} \otimes \hat{h} + \hat{C}$, where $\hat{h} = \mathbf{p}^2/2m^* + V_S(\mathbf{r})$, and $\hat{C} = e^2/4\pi\epsilon_r\epsilon_0|\mathbf{r}_1 - \mathbf{r}_2|$. The tunnelling terms, from the states $\Psi_L^d(\mathbf{r}_1, \mathbf{r}_2)$ or $\Psi_R^d(\mathbf{r}_1, \mathbf{r}_2)$ to $\Psi_0^s(\mathbf{r}_1, \mathbf{r}_2)$, are then given by the matrix element

$$\hbar\Gamma^{(2)} = \sqrt{2}\langle \Phi_{L/R} | \hat{h} | \Phi_{R/L} \rangle + \langle \Psi_{L/R}^d | \hat{C} | \Psi_0^s \rangle, \quad (20)$$

where we have defined a two-electron tunnelling rate, $\Gamma^{(2)}$, including the Coulomb repulsion. If there is no Coulomb repulsion and we ignore the presence of the second electron, we have the ‘bare’ tunnelling rate

$$\hbar\Gamma = \langle \Phi_{L/R} | \hat{h} | \Phi_{R/L} \rangle, \quad (21)$$

$$= \frac{1}{\mathcal{N}^2} [(1 + g^2)w - 2gu], \quad (22)$$

where we have used $w = \langle L | \hat{h} | R \rangle = \langle R | \hat{h} | L \rangle$ and $u = \langle L | \hat{h} | L \rangle = \langle R | \hat{h} | R \rangle$. Furthermore, we find

$$w = \left(1 - \sqrt{\frac{\eta}{\pi}}\right) e^{-\eta} \hbar\omega_0 \quad (23)$$

and,

$$u = \left(1 - \sqrt{\frac{\eta}{\pi}} e^{-\eta} + \eta \operatorname{erfc}(\sqrt{\eta})\right) \hbar\omega_0, \quad (24)$$

where $\operatorname{erfc}(\sqrt{\eta})$ is the complementary error function.

The charging energy, E_C , is approximately the difference in energy between having two electrons in the lowest energy level of a single quantum dot and having only one electron in the dot,

$$E_C \approx E_0^{(2)} - E_0^{(1)}, \quad (25)$$

where $E_0^{(1)}$ ($E_0^{(2)}$) is the ground state energy of 1 (2) electrons in a single harmonic potential. For a single electron in a harmonic trap, as above, $E_0^{(1)} = \hbar\omega_0$. Two electrons in a single harmonic potential is more complex since the Coulomb repulsion of the two electrons must be considered, and in the double quantum dot model above, we have

$$E_0^{(2)} = 2\langle \Phi_{L/R} | \hat{h} | \Phi_{L/R} \rangle + \langle \Psi_{L/R}^d | \hat{C} | \Psi_{L/R}^d \rangle \quad (26)$$

$$= \frac{2}{\mathcal{N}^2} [(1 + g^2)u - 2gw] + U \quad (27)$$

for two electrons on either the left or right quantum dot—these are equivalent. The second term in this model is the onsite interaction in the Hubbard model, U . For well separated quantum dots, $\eta \gtrsim 1.5$, leading to $u \gg w$ and $g \ll 1$, hence $(1 + g^2) \gg 2g$. For the purposes of the following approximations, it is therefore sufficient to give onsite energy due to the momentum and potential as $\langle \Phi_{L/R} | \hat{h} | \Phi_{L/R} \rangle \approx \hbar\omega_0$ and the onsite Coulomb repulsion as $U \approx U_0$, where

$$\hbar U_0 = \int d\mathbf{r}_1 \int d\mathbf{r}_2 \left[\varphi_{L/R}(\mathbf{r}_1)\varphi_{L/R}(\mathbf{r}_2) \times C(\mathbf{r}_1, \mathbf{r}_2)\varphi_{L/R}(\mathbf{r}_1)\varphi_{L/R}(\mathbf{r}_2) \right], \quad (28)$$

with $C(\mathbf{r}_1, \mathbf{r}_2) = e^2/4\pi\epsilon_r\epsilon_0|\mathbf{r}_1 - \mathbf{r}_2|$. The identity $\frac{1}{|\mathbf{r}_1 - \mathbf{r}_2|} = \frac{2}{\sqrt{\pi}} \int_0^\infty dt \exp\{-t^2(\mathbf{r}_1 - \mathbf{r}_2)^2\}$ [26] can be used to compute U_0 , giving $E_0^{(2)} \approx 2\hbar\omega_0 + c\hbar\omega_0$, where

$c = (e^2/4\pi\epsilon_r\epsilon_0\tilde{a})/\hbar\omega_0$ and $\tilde{a} = \sqrt{2/\pi}a$; c is the ratio of the Coulomb energy ($e^2/4\pi\epsilon_r\epsilon_0\tilde{a}$) to the confinement energy ($\hbar\omega_0$). Overall, the charging energy is therefore $E_C \approx (1 + c)\hbar\omega_0$.

Both η and c are dependent on the confinement frequency ω_0 , as $\eta = \eta_0\omega_0$ and $c = c_0/\sqrt{\omega_0}$, where we have introduced the parameters $\eta_0 = l^2m^*/\hbar$ and $c_0 = \sqrt{\pi m^*/2}e^2/4\pi\epsilon_r\epsilon_0\hbar^{3/2}$. After increasing the confinement potential of a single electron by the charging energy, we have the new ground state frequency $\tilde{\omega}_0 = \omega_0 + E_C/\hbar = (2 + c_0/\sqrt{\omega_0})\omega_0$, leading to a change in the ratio of barrier height to half ground state energy, $\tilde{\eta} = (2 + c_0/\sqrt{\omega_0})\eta$. The change in barrier height is therefore dependent on the initial ground state frequency. Typical parameters for GaAs quantum dots are $m^* = 0.067m_e$, $\epsilon_r = 12.9$, and $\hbar\omega_0 = 3$ meV [27], giving $c_0 = 5.11 \times 10^6$ Hz $^{1/2}$ and $c = c_0/\sqrt{\omega_0} = 2.39$, hence $\tilde{\omega}_0 \approx 4.39\omega_0$ and $\tilde{\eta} \approx 4.39\eta$. Thus, the energetic cost of charging is $E_C \approx 10$ meV.

The parameter regime is such that the onsite interaction is approximately $U \approx 20\Gamma$ and since $U \approx U_0 = c\omega_0$, we find $\hbar U \approx 7.2$ meV and $\hbar\Gamma \approx 360$ μ eV, which are both plausible experimental values [20, 24].

By enforcing $U = 20\Gamma$, numerically we find $\eta = 1.86$ gives the correct ratio of onsite interaction and tunnel coupling, and therefore $\tilde{\eta} = 8.17$. The new tunnel coupling is $\tilde{\Gamma} \approx 0.0039\Gamma$. Thereby effectively freezing the electron hopping as the tunnelling of a single electron would take approximately 250 times as long. If we define freezing the interactions as approximately reducing the tunnel coupling to 1% of having the interactions unfrozen, we would only require an increase of the confinement energy of approximately $0.83E_C$, see Fig. 5.

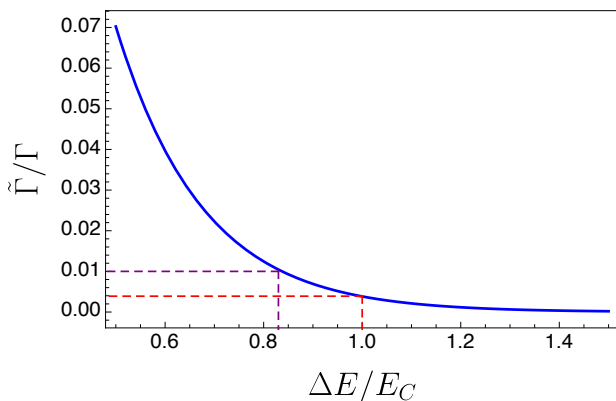


FIG. 5. The ratio of the frozen and unfrozen tunnel couplings against the energy applied, ΔE , to increase the confinement potential (the energy is given in units of the charging energy E_C). The purple dashed line shows that 1% of unfrozen tunnel coupling is achieved for $\Delta E = 0.83E_C$, and the red dashed line shows that 0.4% of unfrozen tunnel coupling for $\Delta E = E_C$.

The preceding applies in the case that there are two electrons. When there is only one electron the charg-

ing energy is significantly less, as we take $c \rightarrow 0$, giving $E_C^{(1)} = \hbar\omega_0$, $\tilde{\omega}_0 = 2\omega_0$, and $\tilde{\eta} = 2\eta$. Assuming the same tunnelling strength of $\hbar\Gamma = 360$ μ eV again leads to $\eta = 1.86$ and therefore the new tunnelling is $\tilde{\Gamma} \approx 0.22\Gamma$, which is much greater than our definition of freezing the tunnelling. In fact, in order to reach the equivalent reduction in tunnelling as in the two-electron case, we must increase the confinement by about $4.5E_C \approx 13.5$ meV. Additional energy is required because with only one electron the confinement potentials are less giving a lower central barrier due to the constant distance between the dots—see Fig. 4.

B. Shuttling

Shuttling is a proposal for transporting electrons in semiconductor devices for scalable quantum computation [14]. An early proposal involves the electron being shuttled by a surface acoustic wave [28]. Subsequent proposals have generally used arrays of quantum dots with tunable metal barrier gates to lower and raise the tunnelling rate between neighbouring dots, inducing a transfer of the electron through the dots sequentially [1, 29–33].

For a fair comparison of the energetics, we assume the quantum dots and spacing between them for shuttling are the same as our state transfer protocol. The energetic cost of shuttling can therefore be considered the sequential loading and unloading of the quantum dots to coherently move the electrons along the chain. Although in practice this may be achieved with a separate barrier potential and raising and lowering the chemical potential of the quantum dots, in the best case, this would be energetically equivalent to freezing and unfreezing the tunnelling between adjacent quantum dots. The energetic cost of shuttling is therefore at least $E_{\text{shuttling}}^{(2)} = 2E_CN \approx 20N$ meV for the two-electron encoding, and $E_{\text{shuttling}}^{(1)} = E_CN \approx 13.5N$ meV for the single-electron encoding.

C. Perfect state transfer scheme

The full energetic cost of our scheme includes freezing and unfreezing interactions, but also the cost of applying the local potential ε_2 for separation and recombination of the electrons (see Fig. 3, steps 1 and 4). The local potentials applied are $\delta \gg \Gamma$, thus as a worst case estimate would change the ground state energies of the electrons by $E_\delta \approx \hbar\delta$. The total energetic cost of our protocol for two-electron encoding is therefore $E_{\text{PST}}^{(2)} = 4E_C + 2E_\delta$, independent of the length of the quantum dot chain N (more accurately, $N + 2$ due to the additional quantum dot required at each end of the chain). In the worst case, $\delta = 40\Gamma$ and therefore $E_{\text{PST}}^{(2)} \approx 108$ meV for the two-electron logical qubit encoding.

A single electron logical qubit encoding would only require the energetic cost of a single step 2 or 3 from Fig. 3. Therefore, we find an energetic cost of $E_{\text{PST}}^{(1)} \approx 54$ meV, half that of the two-electron logical encoding.

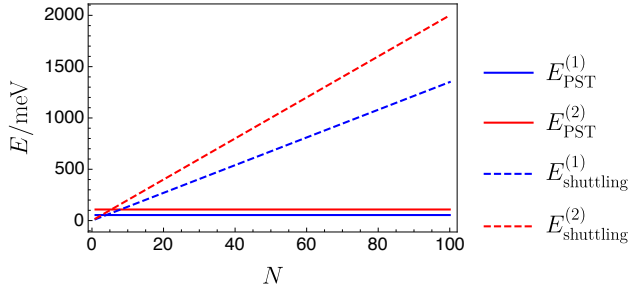


FIG. 6. Comparison of the theoretical energetic costs for the protocol with perfect state transfer (PST) and the shuttling method for logical information with both one and two electron encodings.

D. Lower bound for classical wire

A lower bound for an interconnect in a CPU can be estimated by the energy required to charge the metal wire, CV^2 , where we treat the wire as a capacitor with capacitance $C \sim \epsilon_0 L$, with vacuum permittivity ϵ_0 and L is the length of the wire. The minimal distinguishable voltage is $V \sim k_B T/e$ [13], where k_B is the Boltzmann constant and T is temperature, which we assume to be room temperature because in the cold regime of the quantum dots, we would have to consider the quantum effects of the wire. In the cold regime, we have investigated shuttling instead. The size of quantum dots with 3 meV is approximately 100 nm [27]. Hence, we find the lower bound of $E_{\text{classical}} > 3.7N$ meV, where N is the equivalent number of 100 nm quantum dots for the interconnect. This bound is of course very conservative and in reality far more energy is required in current CPUs, as discussed in the introduction. However, it is already of the same order as quantum coherent buses and, crucially, it scales with N , thus showing the advantage of the perfect state transfer protocol.

VI. NOISE

We have established this advantage in the case that there is no noise. There are several sources of noise for quantum dot qubits. The most significant are nuclear spin noise and charge noise [34, 35]. For tunnelling electrons, another noise contribution is electron-phonon scattering [36–38]. These noise sources particularly contribute dephasing noise, and lead to relatively short T_2 times compared to their relaxation times, T_1 . The coherence times depend on the qubit encoding, with charge qubits having coherence times of $T_1 = 30$ ns

and $T_2 = 7$ ns [39]. For classical information as a low-dissipation classical bus, the dephasing noise is only crucial to maintain coherence for the perfect state transfer part of the protocol. Given a maximum tunnelling rate of $\hbar\Gamma = 360$ μeV , we find that the time for perfect state transfer, $T = (\pi/2)(\hbar/360\mu\text{eV})N \approx 3N$ ps—see Section III. A chain of even 300 ions would still be significantly below the dephasing time of the charge qubits. However, the rate of voltage change required to freeze and unfreeze the chain would therefore be on the order of \sim ps, which is very fast [40]. Reducing the tunnel coupling, and therefore the transfer time, is straightforward by increasing the confinement or increasing the distance between sites. The main source of error would actually be the inability to tune the tunnelling couplings accurately enough for perfect state transfer. The protocol could be applied sequentially, building up perfect state transfer chains such that the distances for each are significantly shorter than the noise that arises from mismatched tunnelling rates. The energetic cost would now be dependent on N , but with a very low prefactor. Even with perfect state transfer chains of only 10 quantum dots would provide an energetic advantage over shuttling. In the case of classical computing, we can disregard the phase information after each perfect state transfer step.

Electrons can be confined in GaAs quantum dots for long times, on the order of seconds [41]. Hence classical bit flip errors are unlikely over the full length of the data bus. Repetition codes can be used to improve the fidelity of bit transmission. The protocol can be performed m times and a majority vote of the outcomes can be used to determine the state.

VII. DISCUSSION

This work considers the energetic cost of state transfer protocols in quantum dot arrays. There are two clear and separate applications for these results. Firstly, to inform the design of quantum dot arrays for quantum computing—in particular, to minimise the on-chip dissipation (heat generation) which imposes demands on the cooling power of the refrigeration—and secondly, as a proposal for the limits of what is possible for energy-efficient data buses for classical information on semiconductor chips.

The perfect state transfer protocols proposed give a theoretical energetic advantage to the current proposals of shuttling electrons. Recent work [14] on scalable quantum computing architectures in quantum dots considered the important issue of power consumption due to the control of a large number of quantum dots and the capacity to cool these devices. Low-dissipation data buses for transferring coherent quantum information would go some way to relaxing this constraint.

Quantum dots and ion-trap chains have both recently been investigated as platforms for a potential energetic advantage in performing classical computations by us-

ing qubits and the coherent evolution of quantum systems [12, 42]. Here, we consider the interconnects, another important and energetically costly component of a universal computer. Using the logical encoding of Ref. [12] for semiconductor quantum dots, we find that perfect state transfer offers a significant energetic scaling advantage compared to a classical data bus. The transfer of information via coherent quantum dynamics for classical data can also reduce a source of energetic overhead

for using reversible quantum devices for classical computation. Without coherent quantum interconnects, the amount of data loading and unloading from classical information could be prohibitively expensive. On the other hand, if a reasonably-sized computational unit, such as an arithmetic-logic unit (ALU), could be implemented with reversible quantum dynamics and quantum coherent data buses, an energetic advantage becomes more attainable.

-
- [1] T. Fujita, T. A. Baart, C. Reichl, W. Wegscheider, and L. M. K. Vandersypen, npj Quantum Information **3**, 1 (2017), number: 1 Publisher: Nature Publishing Group.
- [2] A. M. J. Zwerver, S. V. Amitonov, S. L. de Snoo, M. T. Mađzik, M. Russ, A. Sammak, G. Scappucci, and L. M. K. Vandersypen, “Shuttling an electron spin through a silicon quantum dot array,” (2022), arXiv:2209.00920 [cond-mat, physics:quant-ph].
- [3] H. Qiao, Y. P. Kandel, K. Deng, S. Fallahi, G. C. Gardner, M. J. Manfra, E. Barnes, and J. M. Nichol, (2020).
- [4] S. Bose, Physical Review Letters **91**, 207901 (2003), publisher: American Physical Society.
- [5] M. Christandl, N. Datta, T. C. Dorlas, A. Ekert, A. Kay, and A. J. Landahl, Physical Review A - Atomic, Molecular, and Optical Physics **71**, 032312 (2005), publisher: American Physical Society.
- [6] S. Bose, Contemporary Physics **48**, 13 (2008).
- [7] R. Landauer, IBM Journal of Research and Development **5**, 183 (1961), conference Name: IBM Journal of Research and Development.
- [8] C. H. Bennett, IBM Journal of Research and Development **17**, 525 (1973), conference Name: IBM Journal of Research and Development.
- [9] E. Fredkin and T. Toffoli, International Journal of Theoretical Physics **21**, 219 (1982).
- [10] I. K. Hänninen, C. O. Campos-Aguillón, R. Celis-Cordova, and G. L. Snider, in *Reversible Computation*, Lecture Notes in Computer Science, edited by J. Krivine and J.-B. Stefani (Springer International Publishing, Cham, 2015) pp. 173–185.
- [11] C. O. Campos-Aguillón, R. Celis-Cordova, I. K. Hänninen, C. S. Lent, A. O. Orlov, and G. L. Snider, in *2016 IEEE International Conference on Rebooting Computing (ICRC)* (2016) pp. 1–7.
- [12] J. P. Moutinho, M. Pezzutto, S. Pratapsi, F. F. da Silva, S. De Franceschi, S. Bose, A. T. Costa, and Y. Omar, “Quantum dynamics for energetic advantage in a charge-based classical full-adder,” (2022), arXiv:2206.14241 [cond-mat, physics:quant-ph].
- [13] V. Zhirnov, R. Cavin, and L. Gammaitoni, *Minimum Energy of Computing, Fundamental Considerations* (IntechOpen, 2014) publication Title: ICT - Energy - Concepts Towards Zero - Power Information and Communication Technology.
- [14] J. M. Boter, J. P. Dehollain, J. P. van Dijk, Y. Xu, T. Hensgens, R. Versluis, H. W. Naus, J. S. Clarke, M. Veldhorst, F. Sebastiano, and L. M. Vandersypen, Physical Review Applied **18**, 024053 (2022), publisher: American Physical Society.
- [15] T. Shi, Y. Li, Z. Song, and C.-P. Sun, Physical Review A **71**, 032309 (2005).
- [16] M. B. Plenio and F. L. Semião, New Journal of Physics **7**, 73 (2005).
- [17] A. Wójcik, T. Łuczak, P. Kurzyński, A. Grudka, T. Gdala, and M. Bednarska, Physical Review A **72**, 034303 (2005).
- [18] A. Wójcik, T. Łuczak, P. Kurzyński, A. Grudka, T. Gdala, and M. Bednarska, Physical Review A **75**, 022330 (2007).
- [19] J. Pedersen, C. Flindt, N. A. Mortensen, and A.-P. Jauho, Physical Review B **76**, 125323 (2007).
- [20] T. Hensgens, T. Fujita, L. Janssen, X. Li, C. J. Van Diepen, C. Reichl, W. Wegscheider, S. Das Sarma, and L. M. K. Vandersypen, Nature **548**, 70 (2017), bandiera_abtest: a Cg_type: Nature Research Journals Number: 7665 Primary_atype: Research Publisher: Nature Publishing Group Subject_term: Quantum information; Quantum simulation Subject_term_id: quantum-information; quantum-simulation.
- [21] A. Wensauer, O. Steffens, M. Suhrke, and U. Rössler, Physical Review B **62**, 2605 (2000).
- [22] M. Helle, A. Harju, and R. M. Nieminen, Physical Review B **72**, 205329 (2005).
- [23] Q. Li, Ł. Cywiński, D. Culcer, X. Hu, and S. Das Sarma, Physical Review B **81**, 085313 (2010).
- [24] S. Yang, X. Wang, and S. Das Sarma, Physical Review B **83**, 161301 (2011).
- [25] G. Burkard, D. Loss, and D. P. DiVincenzo, Physical Review B **59**, 2070 (1999).
- [26] K. Singer and M. V. Wilkes, Proceedings of the Royal Society of London. Series A. Mathematical and Physical Sciences **258**, 412 (1960), publisher: Royal Society.
- [27] S. M. Reimann and M. Manninen, Reviews of Modern Physics **74**, 1283 (2002), publisher: American Physical Society.
- [28] S. Hermelin, S. Takada, M. Yamamoto, S. Tarucha, A. D. Wieck, L. Saminadayar, C. Bäuerle, and T. Meunier, Nature **477**, 435 (2011), bandiera_abtest: a Cg_type: Nature Research Journals Number: 7365 Primary_atype: Research Publisher: Nature Publishing Group Subject_term: Quantum dots; Quantum optics Subject_term_id: quantum-dots; quantum-optics.
- [29] T. A. Baart, M. Shafiei, T. Fujita, C. Reichl, W. Wegscheider, and L. M. K. Vandersypen, Nature Nanotechnology **11**, 330 (2016), bandiera_abtest: a Cg_type: Nature Research Journals Number: 4 Primary_atype: Research Publisher: Nature Publishing Group Subject_term: Electronic and spin-

- tronic devices;Nanoscale devices;Qubits;Spintronics
Subject_term_id: electronic-and-spintronic-devices;nanoscale-devices;qubits;spintronics.
- [30] A. R. Mills, D. M. Zajac, M. J. Gullans, F. J. Schupp, T. M. Hazard, and J. R. Petta, *Nature Communications* **10**, 1063 (2019), bandiera_abtest: a Cc_license_type: cc_by Cg_type: Nature Research Journals Number: 1 Primary_atype: Research Publisher: Nature Publishing Group Subject_term: Electronic devices;Quantum dots;Quantum information;Qubits Subject_term_id: electronic-devices;quantum-dots;quantum-information;qubits.
- [31] B. Buonacorsi, B. Shaw, and J. Baugh, *Physical Review B* **102**, 125406 (2020), publisher: American Physical Society.
- [32] F. Ginzl, A. R. Mills, J. R. Petta, and G. Burkard, *Physical Review B* **102**, 195418 (2020), publisher: American Physical Society.
- [33] I. Seidler, T. Struck, R. Xue, N. Focke, S. Trellenkamp, H. Bluhm, and L. R. Schreiber, arXiv:2108.00879 [cond-mat, physics:quant-ph] (2021), arXiv: 2108.00879.
- [34] A. V. Kuhlmann, J. Houel, A. Ludwig, L. Greuter, D. Reuter, A. D. Wieck, M. Poggio, and R. J. Warburton, *Nature Physics* **9**, 570 (2013), number: 9 Publisher: Nature Publishing Group.
- [35] D. Fernández-Fernández, Y. Ban, and G. Platero, *Physical Review Applied* **18**, 054090 (2022), publisher: American Physical Society.
- [36] X. Hu, *Physical Review B* **83**, 165322 (2011), publisher: American Physical Society.
- [37] V. Kornich, C. Kloeffel, and D. Loss, *Physical Review B* **89**, 085410 (2014), publisher: American Physical Society.
- [38] G. He, G. X. Chan, and X. Wang, *Advanced Quantum Technologies* , 2200074 (2023), arXiv:2203.16138 [cond-mat, physics:quant-ph].
- [39] A. Chatterjee, P. Stevenson, S. De Franceschi, A. Morello, N. P. de Leon, and F. Kuemmeth, *Nature Reviews Physics* **3**, 157 (2021), number: 3 Publisher: Nature Publishing Group.
- [40] L. Zou, S. Gupta, and C. Caloz, *IEEE Microwave and Wireless Components Letters* **27**, 467 (2017), arXiv:1610.07115 [physics].
- [41] L. C. Camenzind, L. Yu, P. Stano, J. D. Zimmerman, A. C. Gossard, D. Loss, and D. M. Zumbühl, *Nature Communications* **9**, 3454 (2018).
- [42] S. S. Pratapsi, P. H. Huber, P. Barthel, S. Bose, C. Wunderlich, and Y. Omar, “Classical Half-Adder using Trapped-ion Quantum Bits: Towards Energy-efficient Computation,” (2022), arXiv:2210.10470 [quant-ph].